Effects of Sampling Conditions on the Size Distribution of Fine Particulate Matter Emitted from a Pilot-Scale Pulverized-Coal Combustor

Eric Lipsky,[†] Charles O. Stanier,[‡] Spyros N. Pandis,[‡] and Allen L. Robinson*[,†]

Department of Mechanical Engineering and Department of Chemical Engineering, Carnegie Mellon University, Pittsburgh, Pennsylvania 15213

Received August 2, 2001. Revised Manuscript Received October 17, 2001

A dilution sampler has been designed and manufactured to simulate the effects of dilution processes on particulate matter emissions from coal-fired power plants and other combustion systems. The sampler allows independent control of the dilution ratio and residence time. Experiments were performed to examine the effects of these parameters on the particulate emissions of a pilot-scale pulverized coal combustor burning a low sulfur bituminous coal. Measurements included the particle size distribution in the range from 0.003 to 20 μm and the $PM_{2.5}$ mass emission rate. The residence time and dilution ratio do not influence the particle mass emission rate, but have a significant effect on the size distribution and the total number of particles emitted. Increasing the residence time dramatically decreases the total particle number concentration, and shifts the particle mass to larger sizes. Increasing the dilution ratio increases the concentration of ultrafine particles. The effects of residence time can be explained quantitatively by the coagulation of the emitted particles; however, the effects of dilution ratio are more complex because the dilution ratio influences both the coagulation rate and gas-to-particle conversion.

Introduction

Ambient particulate matter (PM) is a complex mixture of multicomponent particles whose size distribution, composition, and morphology can vary significantly in space and time.[1] Atmospheric PM range in size from a few nanometers to tens of micrometers. Major PM components include sulfates, nitrate, ammonium, and hydrogen ions; trace elements (including toxic and transition metals); organic material; elemental carbon (or soot); crustal components and water.

In 1997 the U.S. Environmental Protection Agency (EPA) promulgated new standards to address ambient air concentrations of PM with an aerodynamic diameter of 2.5 μm ($PM_{2.5}$) because of concerns over human health effects associated with fine particles. The EPA also proposed regional haze regulations for pristine areas in 1997; fine PM is the single greatest contributor to visibility impairment in these areas. Fine PM also plays an important role in climate forcing because of their ability to scatter and absorb light and also because they act as cloud condensation nuclei.[1,2] To reduce the uncertainties regarding the effects of fine PM on human health, visibility, and climate, it is necessary to improve our understanding of physical and chemical properties of atmospheric particles including their size distribution, their number concentration, and their composition. These properties often depend strongly on the source of the PM. PM is emitted directly from sources (primary PM) and is also formed in the atmosphere from reactions of gaseous precursors (secondary PM). Coal-fired utility boilers are a source for both primary PM and gaseous precursors that react in the atmosphere to create secondary PM. This paper examines the size distribution of primary PM emissions from coal combustion.

Numerous investigations have reported measurements of the size distribution of primary PM emissions from coal combustion.[3−8] The results from this work have recently been reviewed.[9] Briefly, primary PM emissions from coal combustion typically have a bimodal distribution.[3,9] The majority of the PM mass occurs in the coarse mode (particles larger than 1 μm); these particles are formed from the fusion and coalescence of inorganic material in the coal.[9] On a number basis, the majority of the PM occurs in the submicron mode with a mean diameter around 0.1 μm; these

* Corresponding author. Tel: (412) 268-3657. Fax: (412) 268-3348. E-mail: alr@andrew.cmu.edu.
[†] Department of Mechanical Engineering.
[‡] Department of Chemical Engineering.

(1) Seinfeld, J. H.; Pandis, S. N. *Atmospheric chemistry and physics: From air pollution to climate change*; John Wiley & Sons Inc.: New York, 1998.
(2) IPCC *Climate Change 1995: The Science of Climate Change*; Cambridge University Press: Cambridge, England, 1996.
(3) McElroy, M. W.; Carr, R. C.; Ensor, D. S.; Markowski, G. R. *Science* **1982**, *215*, 13−19.
(4) Markowski, G. G.; Ensor, D. S.; Hooper, R. G.; Carr, R. C. *Environ. Sci. Technol.* **1980**, *14*, 1400−1402.
(5) Linak, W. P.; Peterson, T. W. *Aerosol Sci. Technol.* **1984**, *3*, 77−96.
(6) Kauppinen, E. I.; Pakkanen, T. A. *Environ. Sci. Technol.* **1990**, *24*, 1811−1818.
(7) Mohr, M.; Ylatalo, S.; Klippel, N.; Kauppinen, E. I.; Riccius, O.; Burtscher, H. *Aerosol Sci. Technol.* **1996**, *24*, 191−204.
(8) Wehner, B.; Bond, T. C.; Mirmili, W.; Heintzenberg, J.; Wiedensohler, A.; Charlson, R. J. *Environ. Sci. Technol.* **1999**, *33*, 3881−3886.
(9) Lighty, J. S.; Vernath, J. M.; Sarofim, A. F. *J. Air Waste Manage. Assoc.* **2000**, *50*, 1565−1618.

10.1021/ef0102014 CCC: $22.00
Published on Web 02/02/2002

particles are formed by vaporization, condensation, and nucleation of inorganic constituents in the fuel.[9,10] The effectiveness of air pollution control devices such as baghouses and electrostatic precipitators at removing particles is size dependent.[9,11] These devices effectively remove coarse mode particles,[3,12,13] but are less effective at controlling submicron particles.[3,7] The exact size distribution of the PM emissions from a coal-fired power plant depends on the coal quality, combustion technology, and the effectiveness of the air pollution control system.

Although much is known regarding the number and mass distribution of PM emitted by coal-fired boilers, a number of issues have yet to be elucidated. These include the importance of the sampling conditions (temperature, dilution ratio, and residence time in the sampling device) on the size distribution and the mass concentration of the emitted particles and the changes to these size distributions as the particles are mixed with ambient air. In addition, relatively little is known of the distribution of ultrafine particles because previous investigations were often limited by the available instrumentation to particles larger than 20−30 nm.

Sampling PM emissions from combustion systems such as coal-boilers is challenging because of the elevated temperatures and high moisture content of the exhaust gases and the inherent complexity of PM. Previous measurements indicate that sampling conditions can alter the measurements of the PM size distribution. For example, Markowski and Filby[14] simultaneously measured the submicron PM size distribution in the stack of a commercial coal-fired boiler with in-stack low-pressure impactors and using a dilution system to extract continuously a sample which was characterized with an electrical mobility analyzer (EAA). The peak of the submicron mode measured using the in-stack impactors was around 0.05 μm while the peak measured by the EAA was around 0.1 μm. Kauppinen and Pakkanen[6] hypothesize that this variation in the peak of the submicron mode may be due to dynamical processes changing the particle size distributions for measurements made on diluted flue gases. Research on emissions from diesel engines has also shown that sampling conditions can alter measured PM size distributions.[15]

The evolution of the PM size distribution in the plume of a power plant must be understood in order to determine the contribution of coal boilers to atmospheric PM. Upon exiting the stack the combustion products are rapidly cooled and diluted with ambient air. During this dilution, aerosol processes such as coagulation, condensation, and nucleation change the size and composition of the PM emissions. Measurements made in plumes using aircraft and at downwind ground sites provide clear evidence that PM emissions from a power plant are altered as the plume mixes with the ambient air.[16−22] For example, gas-to-particle conversion of sulfur species in a coal power plant plume alters the PM size distribution and increases the total mass of PM emissions compared to measurements made in the stack.[16,17,19,21,22] Although aircraft data provide important insight into the evolution of PM in a power plant plume, results from these investigations can often be difficult to interpret because of the inherent complexity of field measurements. In addition, aircraft studies are expensive.

Dilution sampling is a technique that has been developed to examine the influence of rapid cooling and dilution on PM emissions from combustion systems.[23,24] A dilution sampler rapidly mixes hot exhaust gases with a specified amount of conditioned air and allows for processes such as nucleation, condensation, and coagulation to occur. Although a dilution sampler cannot simulate the complexity of actual plume mixing,[25] it allows systematic examination of the effects of dilution on PM emissions in order to better understand the PM transformations that occur in plumes. In particular, dilution samplers are well suited to investigate the transformation that occur in the first seconds to minutes after the exhaust exits the stack. Data regarding the effects of dilution on PM emissions are needed to evaluate theoretical models developed to simulate power plant plumes.[26−29]

Many previous investigations have employed some form of dilution sampling to characterize emissions from coal-fired power plants. The motivation for much of this work was to enable PM size distribution measurements using instrumentation that cannot operate under stack conditions such as EAA, differential mobility analyzers (DMA), or scanning mobility particle sizers (SMPS).[3,4,8,14] The objective of these studies was to measure size distributions, not to examine the effects of dilution on the emissions. Several investigations have also used dilution samplers to collect samples to determine the chemical composition of the PM emissions.[30−32]

(10) Linak, W. P.; Wendt, J. O. L. *Fuel Process. Technol.* **1994**, *39*, 173−198.
(11) Flagan, R. C.; Seinfeld, J. H. *Fundamentals of Air Pollution Engineering*; Prentice Hall: Englewood Cliffs, NJ, 1988.
(12) Ylatalo, S. I.; Hautanen, J. *Aerosol Sci. Technol.* **1998**, *29*, 17−30.
(13) Shendrikar, A. D.; Ensor, D. S.; Cowen, S. J.; Woffinden, G. J.; McElroy, M. W. *Atmos. Environ.* **1983**, *17*, 1411−1421.
(14) Markowski, G. R.; Filby, R. *Environ. Sci. Technol.* **1985**, *19*, 796−804.
(15) Abdul-Khalek, I.; Kittelson, D.; Brear, F. *SAE Technol. Pap. Ser.* **1999**, *No. 1999-01-1142*, 563−571.
(16) Cantrell, B. K.; Whitby, K. T. *Atmos. Environ.* **1978**, *12*, 323−333.
(17) Luria, M.; Olszyna, K. J.; Meagher, J. F. *J. Air Pollut. Control Assoc.* **1983**, *33*, 483−487.
(18) Ondov, J.; Choquette, C.; Zoller, W.; Gordon, G.; Biermann, A.; Heft, R. *Atmos. Environ.* **1989**, *23*, 2193−2204.
(19) Mueller, S. F.; Imhoff, R. E. *Atmos. Environ.* **1994**, *28*, 595−602.
(20) Kim, D. S.; Hopke, P. K.; Casuccio, G. S.; Lee, R. J.; Miller, S. E.; Sverdrup, G. M.; Garber, R. W. *Atmos. Environ.* **1989**, *23*, 81−84.
(21) Gillani, N. V.; Kohli, S.; Wilson, W. E. *Atmos. Environ.* **1981**, *15*, 2293−2313.
(22) Whitby, K. T.; Cantrell, B. K.; Kittelson, D. B. *Atmos. Environ.* **1978**, *12*, 313−321.
(23) Hildemann, L.; Cass, G. R.; Markowski, G. R. *Aerosol Sci. Technol.* **1989**, *10*, 193−204.
(24) England, G.; Toby, B.; Zilinska, B. Critical review of source sampling and analysis methodologies for characterizing organic aerosol and final particulate source emission profiles. Report API 344; American Petroleum Institute: Washington DC, 1998.
(25) Builtjes, P. J. H.; Talmon, A. M. *Boundary-Layer Meteorology* **1987**, *41*, 417−426.
(26) Kerminen, V. M.; Wexler, A. S. *Atmos. Environ.* **1995**, *29*, 361−375.
(27) Damle, A. S.; Ensor, D. S.; Sparks, L. E. *Atmos. Environ.* **1984**, *18*, 435−444.
(28) Meng, R. Z.; Karamchandani, P.; Seigneur, C. *J. Air Waste Manage. Assoc.* **2000**, *50*, 869−874.
(29) Mueller, S. F.; Imhoff, R. E. *Atmos. Environ.* **1994**, *28*, 603−610.
(30) Eatough, D.; Eatough, M.; Lamb, J.; Lewis, L.; Lewis, E.; Eatough, N.; Missen, R. *Atmos. Environ.* **1996**, *30*, 269−281.

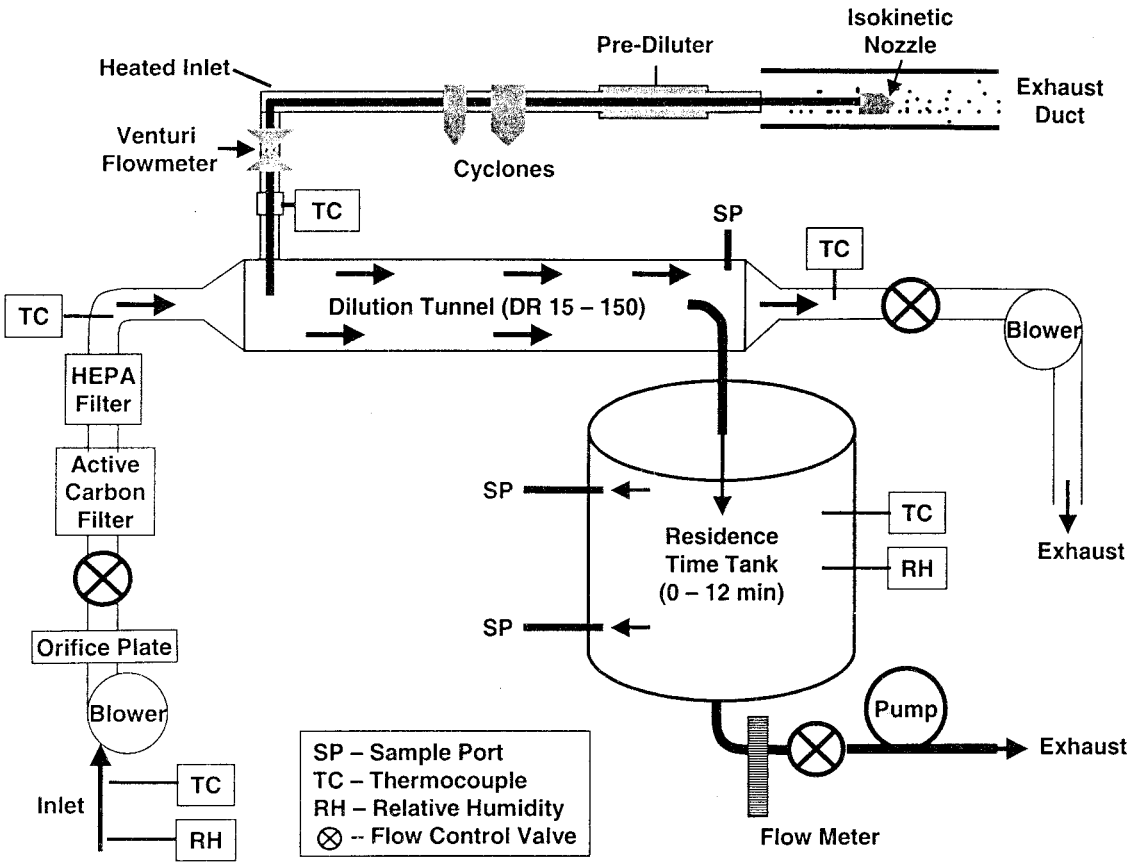

Figure 1. Schematic of the CMU dilution sampler.

This paper aims to improve our understanding of the influence of dilution processes on the size distribution of PM emitted from coal-fired boilers. A dilution sampler was designed and constructed to allow independent control of dilution ratio and residence time. This sampler was installed upstream and downstream of the baghouse of a pilot-scale pulverized coal combustor. Measurements of particle size distributions from 0.003−20 μm were made for a range of dilution ratios and residences times. Filter samples of $PM_{2.5}$ were also collected for gravimetric analysis. The data are compared to predictions from coagulation theory to investigate the influence of aerosol processes on the particle size distribution.

Dilution Sampler Design and Characterization

Figure 1 shows a schematic of the Carnegie Mellon University (CMU) dilution-sampling system (henceforth referred to as the CMU sampler) developed for this investigation. The design is based on the Caltech dilution sampler,[23] with improvements that allow for the independent control of dilution ratio and residence time to allow investigation of the effects of these parameters on emissions. England et al.[24] outline the design criteria for dilution samplers and review previous designs.

The CMU sampler consists of three major components: the sample inlet line, the dilution tunnel, and the residence time tank. Combustion products are isokinetically drawn from the exhaust duct through the sample inlet line, and then turbulently mixed with conditioned ambient air in the dilution tunnel, a 15-cm-diameter, 2.3-m-long stainless steel tube. At the end of the dilution tunnel, a slipstream of this mixture is drawn continuously through the residence time tank. Sampling ports for aerosol characterization instrumentation and filter packs are located at the end of the dilution tunnel and at various locations on the residence time tank. The performance specifications for the sampler are listed in Table 1. All of the parts of the sampler in contact with the exhaust sample and the diluted mixture are made of stainless steel with Teflon gaskets to reduce contamination.

Table 1. Performance Characteristics of Dilution Sampler

parameter	range
dilution ratio	20−200
sample flow	10−30 L/min
dilution air flow	350−1400 L/min
residence time	0−12 min
Reynolds number of flow through tunnel	3000−13000

The flow through the system is controlled with blowers and valves located before and after the dilution tunnel, and after the residence time tank. A slight imbalance between the primary flows into and out of the tunnel draws the combustion products through the inlet sample line and into the dilution tunnel. The flow rate through the sample inlet line is measured directly using a venturi flow meter. The flow rate of the dilution air into the tunnel is monitored using an orifice plate. The dilution ratio is defined as the ratio of volumetric

(31) Pinto, J. P.; Stevens, R. K.; Willis, R. D.; Kellogg, R.; Mamane, Y.; Novak, J.; Santroch, J.; Benes, I.; Lenicek, J.; Bures, V. *Environ. Sci. Technol.* **1998**, *32*, 843−854.

(32) Olmez, I.; Sheffield, A. E.; Gordon, G. E.; Houck, J. E.; Pritchett, L. C.; Cooper, J. A.; Dzubay, T. G.; Bennett, R. L. *JAPCA*—The Int. J. Air Pollut. Control Hazardous Waste Manage. **1988**, *38*, 1392−1402.

flow rate of the dilution air into the tunnel to the volumetric flow rate of combustion products through the sample inlet line—all flows are corrected to standard conditions, 20 °C and 1 atm.

A computer-based data acquisition system automatically records flow rate, temperature, and relative humidity measurements. Parameters that are continuously monitored are the following: the flow rate of the dilution air into the tunnel; the flow rate through the sample inlet line; the temperature and relative humidity of the dilution air entering the tunnel; the temperature of the combustion products entering the tunnel; the temperature of the mixture leaving the tunnel; and the temperature, relative humidity, and pressure of the mixture inside the residence time tank.

Ambient air used to dilute the combustion products is first passed through an activated carbon prefilter to remove organic vapors and a HEPA prefilter to remove particles in the air. Cleaning the dilution air is needed to minimize potential contamination from particles and gases in the ambient air. System blank tests were performed at least once a day and periodically between experiments to verify the cleanliness of the dilution air. During this test, the sample inlet line is closed off and ambient air cleaned by the HEPA and activated carbon prefilters is passed through the system. The cleanliness of the sampler is then evaluated by measuring the particle size distribution at each of the sampling ports and collecting filters for gravimetric analysis. This test identifies contamination from leaks, imperfect performance of the inlet HEPA filter, and entrainment of particles previously deposited on system walls. For the results reported here, system blank levels were always less than 2% of ambient conditions on both a mass and number basis.

Before deploying the CMU sampler, mixing experiments using carbon dioxide as a tracer were performed to verify that the combustion products and ambient air are well mixed by the end of the dilution tunnel across the full range of operational conditions. The sample and dilution air are mixed by turbulence, and the mixing rate depends on the flow rate of the dilution air and the Reynolds number of the flow through the tunnel. At the lowest dilution air flow rate (350 L/min), the Reynolds number of the flow through the tunnel is ~3200, and the sample is well mixed 2.2-m downstream of the inlet, ~9 s after entering the tunnel. At the highest dilution air flow rate (1400 L/min), the Reynolds number of the flow through the tunnel is ~13000, and the sample is well mixed 0.75-m downstream of the inlet, ~0.33 s after entering the tunnel.

A cyclone (Andersen Instruments Series 280 CYCLADE in-stack cyclone) installed on the inlet line removes particles larger than 2.5 μm from the system. Removing particles greater than 2.5 μm reduces particle losses; experiments performed by Hildemann et al.[23] indicate significant losses of large particles in the sample inlet line and venturi flow meter of the Caltech dilution sampler. For the experiments described here, the cyclone was installed on the inlet line immediately outside of the exhaust duct because the exhaust duct of the pilot-scale combustor was not large enough to accommodate the cyclone. For high dilution ratio experiments, a first-stage diluter is added to the inlet line to dilute the combustion products with conditioned ambient air heated to the exhaust temperature. The entire inlet line, including the first-stage diluter and the cyclones, is heat traced and kept at a temperature slightly above the stack temperature to prevent cooling of the sample before the dilution tunnel and to minimize losses due to thermophoresis.

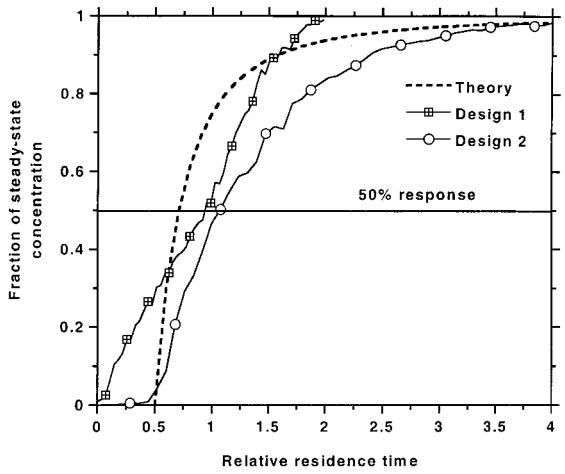

Figure 2. Measurements and theoretical predictions of distribution of transit times of flow through the residence time tank. Measurements are shown for both residence time tank designs. The curves with symbols indicate the carbon dioxide concentrations measured at a sample port during a residence time tank tracer experiment normalized by the steady-state concentration. Results are presented in terms of relative residence time, which is time divided average residence time (time to achieve a 50% response). The theoretical calculations assume fully developed laminar flow through a circular tube.

The residence time tank is a 76-cm-diameter, 91-cm-tall stainless steel cylindrical tank. The flow through the tank is controlled independently using a separate pump and valve system to allow the diluted sample to remain in the tank for a specified time ranging from 0.5 to 12 min. Two different residence time tank designs were used in this study. The first configuration consists of an inlet through the top of the tank, and a set of sample ports located at the bottom of the tank. In the second design, the flow path through the tank was lengthened by installing a 70-cm-long, 38-cm-diameter stainless steel tube inside the tank. In this configuration the diluted sample enters through the center of the top of the tank, passes downward through the inner cylinder, and then flows upward outside the annulus between the inner cylinder and the tank wall. In the second design, sample ports are installed at both the top and bottom of the tank to allow samples to be taken simultaneously at one-half and full residence times.

Tracer experiments were performed using carbon dioxide to characterize the sample transit time through the residence time tank. These experiments consisted of initially operating the sampler on air, and then at time zero injecting carbon dioxide heated to 150 °C (a typical stack temperature) through the sample inlet line at 20 L/min (a typical exhaust sample flow rate). The concentration of carbon dioxide was then monitored at each sample port. The experiment was concluded when the carbon dioxide concentration at the sample port reached a steady-state value.

Results from two residence time tank tracer experiments are shown in Figure 2; initially the carbon dioxide

concentration at a sample port is zero, after a period of time the concentration increases, eventually reaching a steady-state value. This carbon dioxide response curve indicates the distribution of residence times over which a small volume of sample entering the residence time tank reaches a sample port. The fact that the carbon dioxide concentration does not undergo an instantaneous step change between zero and the steady-state value indicates that a single residence time (for example, the ratio of tank volume to flow rate through the tank) does not capture the complexity of the actual flow through the tank. To facilitate comparison between different experimental conditions, we define an average residence time as the time it takes for the carbon dioxide concentration at a sample port to reach 50% of its steady-state value.

Figure 2 shows results from residence time tank tracer experiments performed on each tank design. The performance of the first design is relatively poor because there is almost no delay before the carbon dioxide concentration at the sample port begins to increase. This indicates a fast path through the tank allows a portion of the sample to pass rapidly through the tank. A set of experiments on the pilot-scale coal combustor was performed with this first design. The second design has improved performance, which is much closer to that of theoretical predictions assuming parabolic laminar flow through a circular tube.[33]

Experimental Setup and Procedure

Measurements were performed on the exhaust of the Combustion and Environmental Research Facility (CERF) at the Department of Energy National Energy Technology Laboratory. The CERF is a pilot-scale pulverized coal combustor that simulates the time−temperature history of a commercial coal boiler. At full load it consumes 20 kg of pulverized coal per hour, roughly 150 kW when burning a U.S. bituminous coal. Coal is injected through a swirl-stabilized burner at the top of a 3-m-tall and 45-cm-diameter refractory lined combustion zone. Combustion products then flow into a horizontal convective section, through two flue gas coolers, heat-traced piping, and into a bag-house. The CERF was operated on Prater Creek coal, an eastern bituminous coal with low ash and low sulfur content. Results from standard analyses of the coal are shown in Table 2.

Experiments were conducted to examine the effects of dilution ratio and residence time on the PM size distribution and PM mass emission rate while the CERF was operated at constant conditions. Two types of experiments were performed: (1) the residence time was held constant while the dilution ratio was varied, and (2) the dilution ratio was held constant while varying the residence time. One week of particle size distribution measurements were made before the bag-house using the first residence tank design. This configuration required adjusting the flows to change the residence time in the system. Two weeks of testing were conducted with the second tank design: one week of particle size measurements after the bag-house, and one week of filter samples before the bag-house. This second design allows simultaneous measurements at multiple residence times, which minimizes the effects of operational variability of the CERF on the data.

Measurements of particle size distribution from 0.003−20 μm are made using sizing instrumentation connected to the sample ports on the dilution tunnel and residence time tank.

Table 2. Composition of Prater Creek Coal

Proximate Analysis

parameter	wt %, as rcvd
moisture	2.0
volatile matter	38.7
fixed carbon	54.5
ash	4.7
HHV (BTU/lb)	14167

Ultimate Analysis

parameter	wt %, dry basis
hydrogen	5.4
carbon	78.3
nitrogen	2.3
sulfur	0.8
oxygen (diff)	8.4
ash	4.7

Ash

parameter	wt %, ash basis
SiO_2	38.4
Al_2O_3	25
Fe_2O_3	23.5
TiO_2	1.0
P_2O_5	0.1
CaO	3.8
MgO	2.1
Na_2O	0.3
K_2O	2.2
SO_3	4.6

One Scanning Mobility Particle Sizer (SMPS) measures particles between 0.003 and 0.075 μm (TSI model 3085 Electrostatic Classifier with a TSI model 3025 CPC). A second SMPS measures particles from 0.015−0.65 μm (TSI model 3081 Electrostatic Classifier with a TSI model 3010 CPC). An Aerodynamic Particle Sizer (APS) measures particles in the range of 0.5−20 μm, overlapping with the second SMPS (TSI model 3320). Two neutralizers are used in series before both of the SMPS analyzers to ensure a known charge on the particles. Further dilution of the sample flow was required under certain conditions to lower concentrations of the particles below maximum detection levels of the CPC.

Filter samples were collected to examine the effect of dilution ratio and residence time on PM mass emission rates. The filter samples were collected at the end of the dilution tunnel and at different locations on the residence time tank; no filter samples were collected at stack conditions. The samples were collected on 47-mm, 2-μm Teflo filters (Gelman Corp). The filters were equilibrated for at least 24 h and weighed in a temperature (21−23 °C) and relative humidity (30−40%) controlled glovebox following standard EPA protocols.

All of the results are reported on a unit exhaust volume basis of the pilot-scale combustor at standard temperature and pressure. This allows direct evaluation of the effects of dilution and residence time on actual emissions, and facilitates comparison of data collected at different dilution ratios.

Coagulation Model

A coagulation model was used to simulate the changes over time of the particle size distribution within the residence time tank to better understand the effects of dilution and residence time on the measured size distributions. These calculations were performed using a model previously described by Capaldo et al.[34] with only the coagulation term active. This model describes

(33) Folger, H. S. *Elements of Chemical Reaction Engineering*, 2nd ed.; Prentice Hall: Englewood Cliffs, NJ, 1992.

(34) Capaldo, K. P.; Kasibhatla, P.; Pandis, S. N. *J. Geophys. Res.—Atmos.* **1999**, *104*, 3483−3500.

the evolution of the aerosol size distribution of an isolated air parcel with time. Briefly, the aerosol size distribution is divided into a number of equal size sections, with N_k representing the number concentration of particles in section k. The evolution of an aerosol size distribution by coagulation can then be described by[1]

$$\frac{dN_k}{dt} = \frac{1}{2}\sum_{j=1}^{k-1} K_{j,k-j}N_jN_{k-j} - N_k\sum_{j=1}^{\infty} K_{k,j}N_j \quad k \geq 2 \quad (1)$$

where dN_k/dt is the rate of change in number concentration of particles in section k with time, $^1/_2\ \sum_{j=1}^{k-1} K_{j,k-j}N_jN_{k-j}$ is the formation rate of new particles in section k due to collision of smaller particles, and $N_k\ \sum_{j=1}^{\infty} K_{k,j}N_j$ is the depletion rate of particles in section k due to collision of particles in section k with other particles. The parameter $K_{k,j}$ is the coagulation coefficient between particles in section k and j. For these calculations the coagulation coefficient was determined assuming coagulation occurs only by Brownian motion. The Brownian coagulation coefficient depends on the properties of the air and size of the particles in each section, and was evaluated using the procedures described by Seinfeld and Pandis.[1]

The model solves eq 1 using an initial aerosol size distribution determined by fitting a three-mode lognormal size distribution to the measurements made at the end of the dilution tunnel (0 residence time). The model then divides this distribution into 150 equal-sized sections.

The model was used to simulate the changes in the particle size distribution as the sample passes through the residence time tank. The model assumes that the air parcels within the tank do not mix. To account for the nonuniform flow through the residence time tank (see Figure 2), calculations were performed for 10 different air parcels each with the same initial size distribution. Each of these parcels was aged for different periods of time. The results from each of these calculations were then combined using a weighted average to account for the different sample transit times through the tank to estimate the particle size distribution at a sample port. The weights for this calculation were determined by the residence time distribution measured by the carbon dioxide tracer studies (see Figure 2).

Results

Figure 3 presents size distributions on both a particle number and a particle volume basis measured before and after the bag-house at a residence time of 1.5 min and a dilution ratio 70. The particle mass distribution will be very similar to that of the particle volume shown in Figure 3b because particle density is typically not a strong function of particle diameter. The emissions on a volume (and mass) basis are dominated by particles greater than 1 μm; the emissions on a number basis are dominated by particles smaller than 100 nm. Comparing the size distributions measured before and after the bag-house reveals that the bag-house significantly reduces the emissions of both particle number and mass.

Three modes can be seen in the particle size distribution measured before the bag-house; only two modes are present in the size distribution measured after the bag-house. A coarse mode that peaks around 2 μm is present before and after the bag-house; these are residual fly ash particles formed from the fusion and coalescence of mineral matter in the coal. Note that the experiments before the bag-house only measure the lower end of the residual fly ash mode because the cyclone on the inlet line removes particles greater than 2.5 μm. A fine mode around 0.05 to 0.1 μm can also be seen before and after the bag-house, which is formed from the condensation and nucleation of metals volatilized during the combustion process. The presence of these two modes is consistent with previously reported measurements of particle size distributions in coal combustion.[3−9]

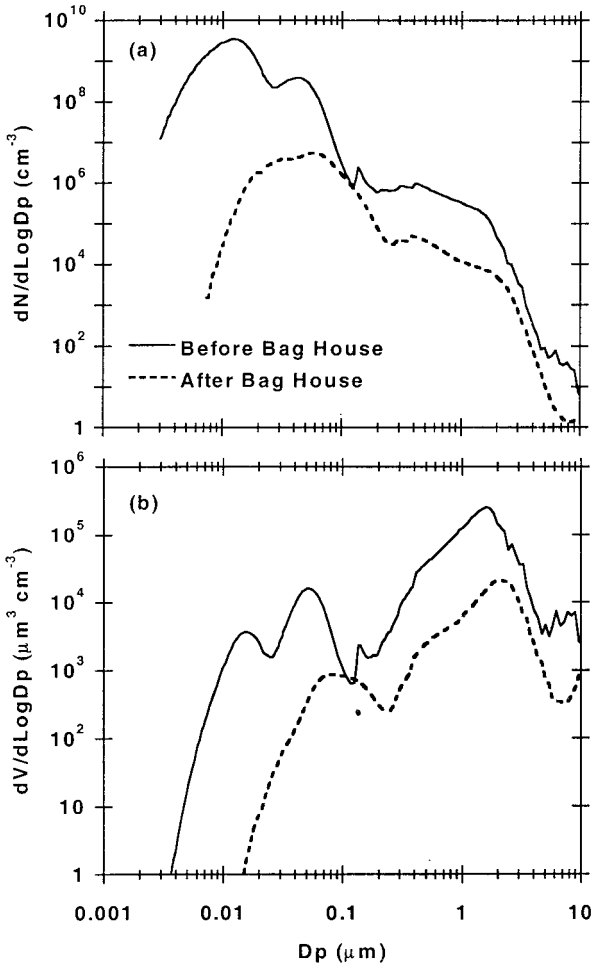

Figure 3. Typical particle (a) number and (b) volume distributions measured before and after the bag-house at a dilution ratio of 70 and a residence time of 1.5 min. Concentrations are reported on a unit exhaust volume basis of the pilot-scale combustor corrected to standard temperature and pressure.

The particle size distribution measured before the bag-house also contains an ultrafine mode with a peak around 0.01 μm. The particles in this mode dominate the emissions of particle number, but contribute negligibly to the emissions of particle volume (and mass). This mode is probably a sulfuric acid fume, which formed from the reaction of SO_3 and H_2O and the condensation and nucleation of H_2SO_4 as the combustion products rapidly cool in the dilution tunnel.[11,27,29] The ultrafine mode is not observed after the bag-house—only one brief nucleation event was recorded during the week of sampling after the bag-house. We suspect that

the absence of the ultrafine mode after the bag-house is due to the removal of the SO_3 in the exhaust as the flue gas passes through the bag. In addition, the removal efficiency to the bag should be high for these ultrafine particles. The presence of an ultrafine mode has been previously reported.[7,35] However, previous investigations, because of instrumentation limitations, have not been able to measure particles less than about 0.02 μm, and the presence of an ultrafine mode has been determined based on extrapolations from measurements made at larger particle sizes.[7] Using similar instrumentation as that employed here, Wehner et al. report measurements of particle size down to 0.003 μm, but did not observe an ultrafine mode.[8]

Figure 4 shows the evolution of the size distribution as a function of residence time. These distributions were measured before the bag-house at a constant dilution ratio of 70, and residence times of 0, 1.5, and 12 min. The initial (zero time) residence time distribution is measured at the end of the tunnel before the diluted sample enters the residence time tank. The data indicate that changing the residence time alters the size distribution of the submicron particles, but has no effect on the distribution of particles greater than 1 μm. Increasing the residence time reduces the particles in the ultrafine 0.01 μm mode; this reduction is especially dramatic during the first minute. Increasing the residence time also shifts 0.05 μm mode toward larger particle sizes.

Changing the dilution ratio also alters the size distribution of the submicron particles. Figure 5 presents size distributions measured before the bag-house at a constant residence time and dilution ratios of 15, 70, and 150. Increasing the dilution ratio increases the particle number, especially in the ultrafine 0.01-μm mode. Changing the dilution ratio does not affect the size distribution of particles greater than 1 μm.

Figure 6 presents $PM_{2.5}$ mass emission rate data determined from gravimetric analysis of the filter samples collected before the bag-house. For each experiment, filter samples were collected simultaneously at three different residence times; the data were then normalized by the average mass emission rate for a given experiment to facilitate comparison between different experiments. The average $PM_{2.5}$ mass emission rate before the bag-house was 1.9 g/kg coal.

The dilution ratio and residence time do not influence $PM_{2.5}$ mass emission rate, indicating that there is no significant transfer of mass via nucleation or condensation occurring within the residence time tank. This is not unexpected because of the low levels of volatile species in coal combustion exhaust. As the combustion products rapidly cool and dilute inside the dilution tunnel, the SO_3 in the exhaust stream will react with H_2O to form H_2SO_4 that will subsequently condense or nucleate to create new aerosol mass.[11,27,29] These reactions are very rapid and will likely be complete before the sample enters the residence time tank. It is unlikely that additional SO_2 in the exhaust would oxidize inside the residence time tank because oxidant concentrations (e.g., OH or O_3) in combustion products are typically very low.[36] Aircraft-based studies have shown significant gas-to-particle conversion in plumes due to oxidation of SO_2 downwind from a power plant.[16,17,19,21,22] In this situation the SO_2 is oxidized as the plume mixes with polluted ambient air. Condensation of semi-volatile organics can increase particle mass in the residence time tank,[23] but the concentration of these species in coal combustion is very low.[37−40] Plume data also suggests gas-to-particle conversion of semi-volatile trace metals such as selenium and arsenic;[18,41] however, these

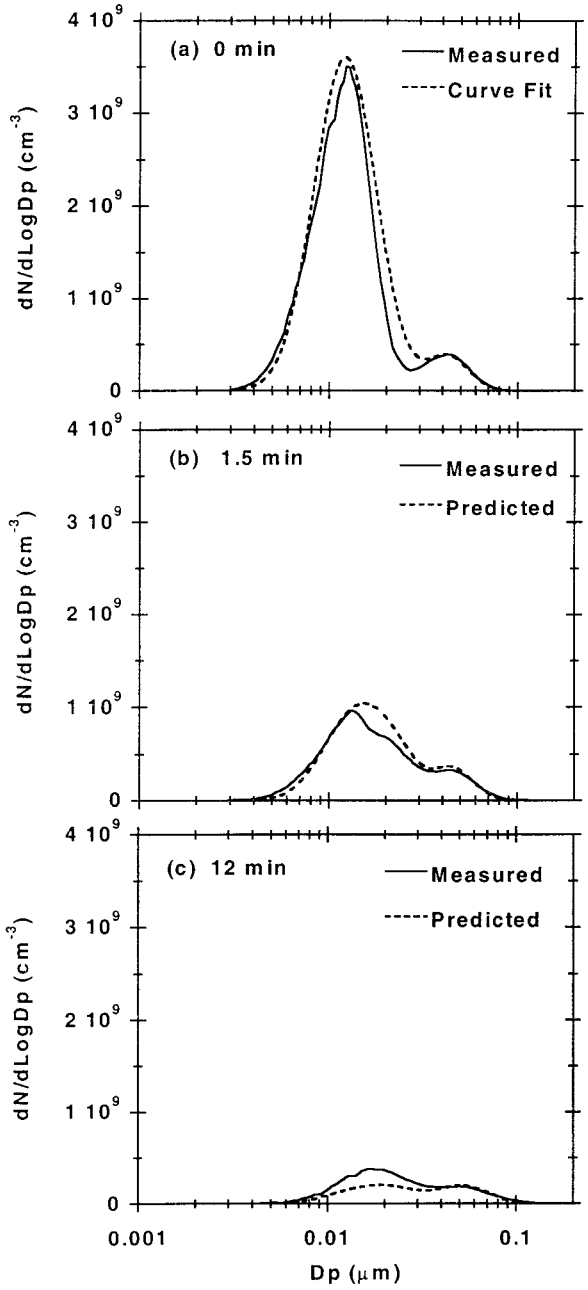

Figure 4. Change in particle size distribution with residence time at a dilution ratio of 70. Predictions based on coagulation theory using a curve fit of the zero residence time measurements as the initial condition. Concentrations are reported on a unit exhaust volume basis of the pilot-scale combustor corrected to standard temperature and pressure. All the distributions are plotted on the same scale to underscore the impact of residence time on the size distribution.

(35) Lind, T.; Kauppinen, E. I.; Maenhaut, W.; Shah, A.; Huggins, F. *Aerosol Sci. Technol.* **1996**, *24*, 135−150.

(36) Karamchandani, P.; Koo, A.; Seigneur, C. *Environ. Sci. Technol.* **1998**, *32*, 1709−1720.

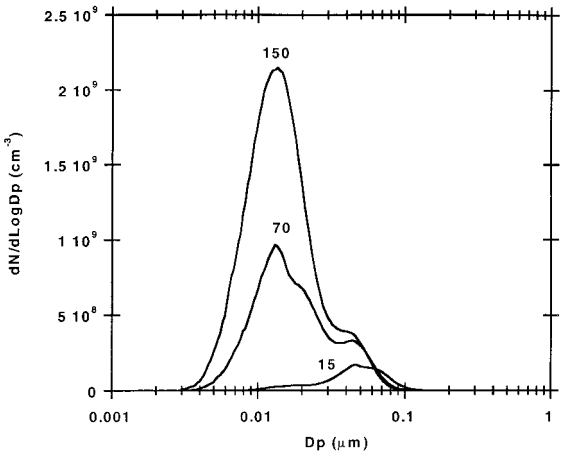

Figure 5. Particle number distributions measured at dilution ratios of 150, 70, and 15 at a residence time of 1.5 min. Concentrations are reported on a unit exhaust volume basis of the pilot-scale combustor corrected to standard temperature and pressure.

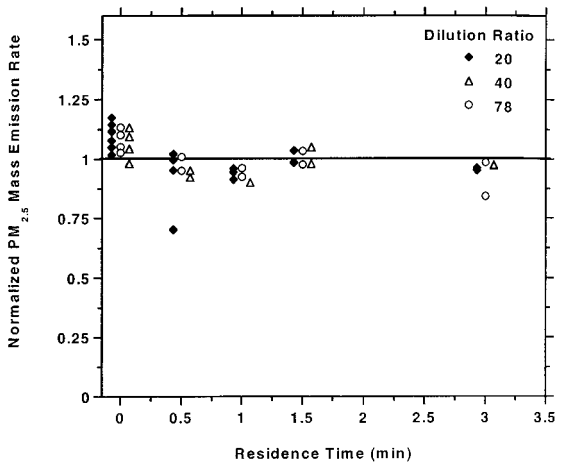

Figure 6. Normalized $PM_{2.5}$ mass emissions as a function of residence time. Measurements were made at four different residence times 0, 0.5, 1, 1.5, and 3 min. The residence times of the symbols indicating the dilution ratio 20 and 40 data have been shifted slightly to improve the visual clarity of the figure.

species are not presented in sufficient quantities to alter the $PM_{2.5}$ mass emission rate.

Dilution ratio and residence time both have a significant impact on the total number of particles emitted. Figure 7 presents total number concentration as a function of residence time and dilution ratio. Increasing the residence time reduces the number concentration; for example, increasing the residence time from 0 to 12 min reduces the particle number by a factor 7 for experiments conducted with a dilution ratio of 70. Increasing the dilution ratio increases the total number concentration; for example increasing the dilution ratio from 15 to 100 increases the number concentration by a factor of 15 for experiments conducted with a residence time of 1.5 min.

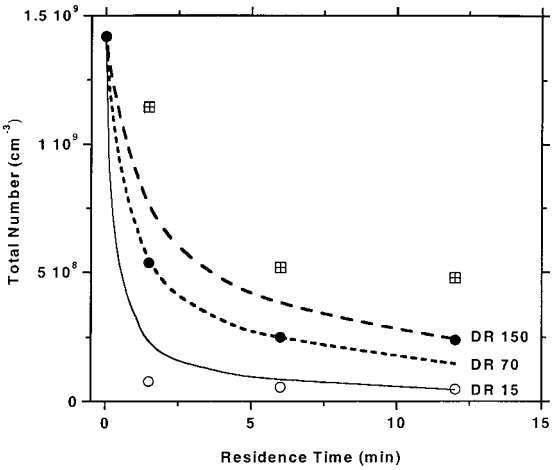

Figure 7. Comparison of measured and predicted total number concentration as a function of residence time. The squares, solid circles, and open circles indicate measured values at dilution ratios of 150, 70, and 15, respectively. The lines represent model calculations at dilution ratios of 15, 70, and 150. Concentrations are reported on a unit exhaust volume basis of the pilot-scale combustor corrected to standard temperature and pressure.

Analysis and Discussion

Predictions of the coagulation model are compared to the measurements to better understand the effects of dilution and residence time on the measured size distributions. The model only accounts for effects of coagulation on the aerosol size distribution. The input for the model is the size distribution measured at the end of the dilution tunnel. The model−measurement comparison shown in Figure 4 indicates that the model reproduces the changes in the particle size distribution with increasing residence time at a given dilution ratio. This agreement suggests that the main process occurring within the residence time tank for these conditions is Brownian coagulation of the emitted particles.

Model predictions are shown in Figures 7 and 8 to examine whether the observed effects of dilution ratio on the total number concentration and size distribution can be explained by changes in the coagulation rate of the particles. Dilution dramatically alters the coagulation rate, which varies with the square of the particle number concentration—see eq 1. If coagulation is the dominant process in determining the effects of dilution then it should be possible to scale a size distribution measured at 0 residence time to any dilution ratio and then use the coagulation model to predict the time evolution of the size distribution at the new dilution ratio. If true, this would significantly simplify sampling requirements because measurements at one dilution ratio could be used to predict emissions at another dilution ratio. To test this hypothesis we scaled the particle concentrations of the measured size distribution at 0 residence time and a dilution ratio of 70 to a dilution ratio of 15 and 150, and used the model to predict the evolution of the total number concentration

(37) Weber, G. F.; Erickson, T. A.; Hassett, D. J.; Hawthorne, S. B.; Katrinak, K. A.; Lousi, P. K. K. A comprehensive assessment of toxic emissions from coal-fired power plants: Phase I results from the U.S. Department of Energy study. Energy & Environmental Research Center: Grand Forks, ND, 1996.

(38) Garcia, J. P.; Beyne-Masclet, S.; Mouvier, G.; Masclet, P. *Atmos. Environ.* **1992**, *26A*, 1589−1597.

(39) Miller, C. A.; Srivastava, R. K.; Ryan, J. V. *Environ. Sci. Technol.* **1994**, *28*, 1150−1158.

(40) Electric utility trace substances synthesis report. Report EPRI TR-104614; Electric Power Research Institute: Palo Alto, CA, 1994.

(41) Eatough, D.; Eatough, M.; Lewis, L.; Lewis, E.; Tomlinson, E.; Gordon, J.; Eatough, N. *Atmos. Environ.* **1996**, *30*, 283−294.

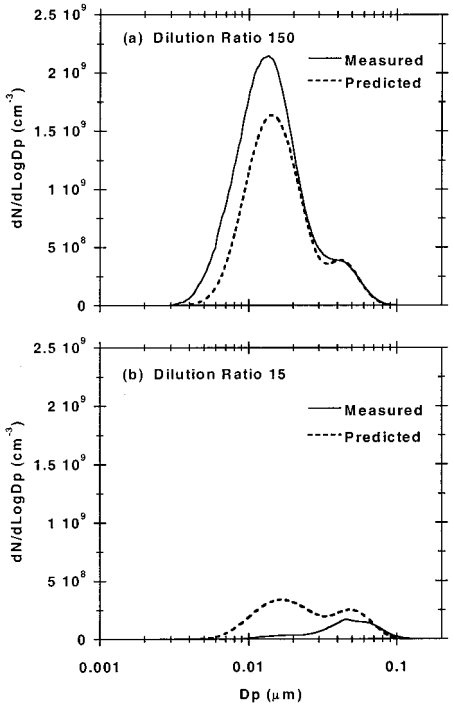

Figure 8. Comparison of measured and predicted size distributions at a residence time of 1.5 min. Concentrations are reported on a unit exhaust volume basis of the pilot-scale combustor corrected to standard temperature and pressure. All the distributions are plotted on the same scale to underscore the impact of dilution ratio on the size distribution.

(Figure 7) and the size distributions (Figure 8) at the new dilution ratios.

Comparing the measurements and model predictions in Figures 7 and 8 reveals that, although the model qualitatively predicts the correct trends, coagulation alone is not sufficient to explain the effects of dilution ratio on the size distribution. For the dilution-ratio-150 case the model underpredicts the number of ultrafine particles and the total number concentration. For the dilution-ratio-15 case the model overpredicts the number of ultrafine particles and the total number concentration, but the predictions of total number concentration become more accurate at longer residence time.

The model measurement comparison in Figures 7 and 8 indicates that, while coagulation is important, at least one other process affects the size distribution of the emitted ultrafine particles. Comparisons of the size distributions measured at the end of the dilution tunnel suggest that these additional processes occur in the dilution tunnel and not the residence time tank. Figure 9 presents size distribution measured at the end of the dilution tunnel at a dilution ratio of 15 and a dilution ratio of 70. A large ultrafine mode can be seen in the size distribution measured at a dilution ratio of 70, but not in the distribution measured at a dilution ratio of 15. This suggests that changing the dilution ratio affects the formation of new particles by nucleation.

Upon entering the dilution tunnel, the combustion products are rapidly diluted and cooled causing SO_3 to react with H_2O to create H_2SO_4, sulfuric acid. The rapid cooling of the combustion products creates a supersaturation of sulfuric acid. Whether or not this material condenses or nucleates to create new ultrafine particles depends on the available particle surface area.[26] The

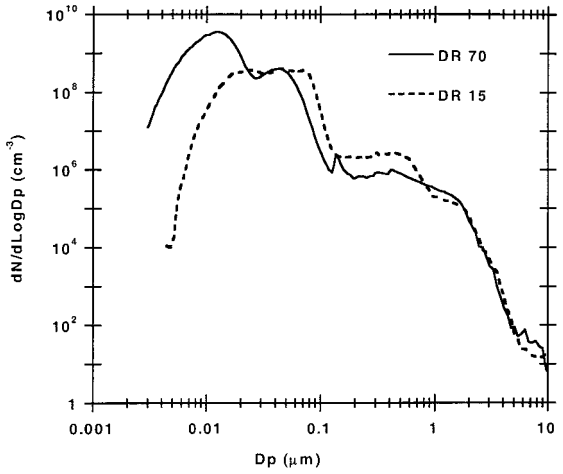

Figure 9. Size distributions measured at the end of the dilution tunnel at dilution ratios of 15 and 70.

lower the dilution ratio the greater amount of surface area per unit volume and the more likely that the sulfuric acid will condense onto existing particles, reducing the production by nucleation of new particles in the ultrafine mode. High dilution ratios reduce the amount of available surface area per unit volume, which increases nucleation and the number of particles in the ultrafine mode. Therefore, one must account for coagulation, nucleation, and condensation when considering the effects of dilution ratio on the particle size distribution. Similar observations regarding the complex relationship between dilution ratio and aerosol size distribution have been made in studies of diesel exhaust particles.[15]

Conclusions

Particle size distributions from 0.003 to 20 μm were measured using a dilution sampler before and after the bag-house of a pilot-scale pulverized coal combustor. Experiments were performed to examine the influence of dilution ratio and residence time on the size distribution and the total number and mass emissions.

The residence time and dilution ratio do not influence the particle mass emission rate but change the size distribution and total number emissions. Increasing the residence time dramatically decreases the total particle number concentration, and shifts the particle mass to larger sizes. Increasing the dilution ratio increases the concentration of ultrafine particles. The effects of residence time can be explained with coagulation theory; however, the effects of dilution ratio are more complex because dilution ratio influences coagulation, condensation, and nucleation. The sensitivity of the particle size distribution and total number of particles emitted to changes in dilution ratio and residence time underscore the challenges associated with measuring and simulating the particle size distribution in the plume of a coal-fired power plant.

Acknowledgment. This work was supported by the U.S. Department of Energy under the University Coal Research Program, Grant DE-FG2699-FT40583. The authors thank M. Freeman, W. O'Dowd, and G. Walbert for their assistance operating the CERF, and Sarah Rees, Tim Raymond, and Cem Cenker at Carnegie Mellon for their assistance with the sampling.

EF0102014